Research Square

Preprints are preliminary reports that have not undergone peer review.
They should not be considered conclusive, used to inform clinical practice,
or referenced by the media as validated information.

Angular resolution of the two-center Dirac equation in Prolate Spheroidal coordinates

Miguel Angel Díaz-Gutiérrez
Universidad Complutense de Madrid
Piero Decleva
University of Trieste
Felipe Zapata
fezapata@ucm.es

Universidad Complutense de Madrid

Research Article

Keywords:

Posted Date: November 24th, 2026

DOI: https://doi.org/10.21203/rs.3.rs-11653416/v1

License: This work is licensed under a Creative Commons Attribution 4.0 International License.
Read Full License

Additional Declarations: No competing interests reported.

Angular resolution of the two-center Dirac equation in Prolate Spheroidal Coordinates

Miguel A. Díaz-Gutiérrez[1,2], Piero Decleva[3,4], and Felipe Zapata[1*]
[1] *Departamento de Química Física, Universidad Complutense de Madrid, 28040 Madrid, Spain*
[2] *Instituto Madrileño de Estudios Avanzados en Nanociencia (IMDEA-Nanociencia), Cantoblanco, 28049 Madrid, Spain*
[3] *Dipartimento di Scienze Chimiche e Farmaceutiche, Università degli Studi di Trieste, via L. Giorgieri 1, 34127 Trieste, Italy and*
[4] *Consiglio Nazionale delle Ricerche - Istituto Officina dei Materiali (CNR-IOM), 34149 Trieste, Italy*

In this work, a complete derivation of the two-center Dirac equation in Prolate Spheroidal coordinates is presented. Different recurrence relations have been derived in order to reach a total angular resolution of the problem. The validity of such recurrence relations has been checked numerically, allowing us to compute the required angular integrals analytically. Finally, we also discuss in details a numerical implementation of the two-center Dirac equation in Prolate Spheroidal coordinates using a basis set composed by B-splines and spherical harmonics. The results of the present work can be directly used to find bound and continuum state solutions, required, for example, in scattering problems or in relativistic electronic structure calculations. Moreover, the utilization of Prolate Spheroidal coordinates allows one to explore striking scenarios with high accuracy. For example, in the investigation of core-level photoionization of heavy molecules.

I. INTRODUCTION

Recent improvements at Free Electron Laser facilities have enable the possibility of investigating core-level photoionization processes in complex molecules at its natural time scales [1–3]. In this regard, the opportunity to explore core-level photoionization in heavy molecules containing atoms such as S, Cl or I, have called for the development of theoretical treatments based on the Dirac equation due to the relativistic nature of the electron dynamics [4]. In such scenarios, the resolution of the molecular Dirac equation becomes crucial. Today, accurate electron bound solutions can be obtained with relativistic quantum-chemistry packages, such as DIRAC [5], BAGEL [6], or semi-relativistic codes, such as ADF [7]. However, there are not so many codes for the treatment of the relativistic molecular continuum. This limitation is associated to the numerical instabilities directly related to the appearance of the so-called "spurious states" [8]. This problem is related to the use of inappropriate boundary conditions when solving the Dirac equation and it is also present in atomic calculations [9]. As a result, these unphysical solutions must be "removed" from the numerical spectrum. Unfortunately, the task of removing the undesired solutions can be very laborious [10], even impracticable in molecular systems due to the complex nature of their electronic spectrum.

In the context of atomic calculations, different approaches have been proposed to avoid the appearance of the spurious states [11–14]. Although, no best method was found at that time, dual kinetic balanced (DKB) basis sets were adapted to solve the one-electron two-center Dirac equation [15–19]. Additionally, we can mention here the early works based on Ellipsoidal coordinates [20–22], the utilization of linear combination of atomic orbitals (LCAO) [23–29] and the direct integration of the equation [30–40], giving access to very accurate bound state solutions [41–43]. In the context of atomic R-matrix calculations, Froese-Fischer and Zatsarinny proposed an alternative approach based on a relativistic B-spline Galerkin method that introduces the correct boundary conditions to the problem [8]. Recently, this numerical method has been extended by Zapata *et al.* [4] to solve the one-electron two-center Dirac equation for both bound and continuum solutions. This recent development opens the door for the investigation of core-level photoionization in heavy molecules and allows us to reproduce angle- and spin-resolved photoelectron spectroscopy (ASRPES)-like experiments from where angle- and spin-resolved information can be extracted.

For the time being, the numerical resolution of two-center Dirac equation given in ref. [4] was based on the so-called "one-center expansion" approximation, where the two-center Coulomb potential is expanded in Spherical coordinates, using the center of charge of the molecule as the one-center expansion origin [44, 45]. The electron wave function is then also expanded over different partial wave components, being centered at the one-center expansion origin. Despite the fact that this approach is quite robust, it is not the most efficient one to investigate molecules containing heavy off-centered atoms, due to its relatively slow convergence [46]. Alternatively, a system of coordinates that naturally takes into account the singularities generated by the two-center Coulomb potential is the so-called Prolate Spheroidal system [47]. Within this system of coordinates, the electron wave function can be split into a "radial" component and an angular term. As a result, the matrix elements of the Dirac Hamiltonian can be also split into radial and angular terms. While the radial terms can be easily evaluated numerically using the implementation given in ref. [4], the angular components can be evaluated analytically. However, the analytical evaluation of such components is very tedious and, to the best of our knowledge, it cannot be found in the literature. In order to cover such a gap, we present here the complete angular resolution of the two-center Dirac equation in Prolate Spheroidal coordinates

*fezapata@ucm.es

in details. The derivations presented hereby are the result of a master thesis work carried out in the context of the TCCM-EM programme between the Universidad Autonoma de Madrid (UAM) and the Universidad Complutense de Madrid (UCM). The structure of the present work is the following one.

In Section II, we present the two-center Dirac equation for a fixed-nuclei diatomic molecule. The Prolate Spheroidal coordinates are introduced and the basis set in such system of coordinates is described. In Section III, the computational details are provided. The required matrix elements for the integration of the two-center Dirac equation are presented. In addition, we discuss a possible numerical implementation of the radial integrals following our previous work in ref. [4]. In Section IV, we derive the recurrence relations needed for the analytical evaluation of the angular integrals involved in the computation of matrix elements. The validity of such recurrence relations has been checked numerically. Here we present a brief proof of such numerical test trough a graphical representation of the recurrence relations. Finally, the expressions for all the required angular integrals involved in the problem are provided in detail. In Section V, a conclusion is given. In this work, atomic units (a.u.) are used unless otherwise stated, $e = \hbar = m_e = 4\pi\epsilon_0 = 1$.

II. THE TWO-CENTER DIRAC EQUATION

One-electron diatomic molecules are characterized by a Coulomb potential of two centers, e.g. A and B with an interatomic distance of R and an electron at point (x, y, z), with distances r_A and r_B from the two nuclei, i.e.

$$r_A = \sqrt{x^2 + y^2 + (z+a)^2}; \tag{1a}$$

$$r_B = \sqrt{x^2 + y^2 + (z-a)^2}, \tag{1b}$$

where $a = R/2$. The Coulomb potential in Cartesian coordinates is then given by the following expression.

$$V_{\rm TC}(r_A, r_B) = -\frac{Z_A}{r_A} - \frac{Z_B}{r_B}, \tag{2}$$

Z_A and Z_B being the nuclear charges. As a result, the associated two-center Dirac problem presents cylindrical symmetry. In this regard, the z-component of the total angular momentum, J_z, is a constant of motion,thus m is a good quantum number, allowing us to classify the one-electron 4-component molecular orbitals $|\psi_m\rangle$ by means of $|m| = \frac{1}{2},\ \frac{3}{2},\ \frac{5}{2}...$ [48]. This fact also allows us to write the two-center Dirac equation as follows,

$$H|\psi_m\rangle = E|\psi_m\rangle, \tag{3}$$

E being the energy of the one-electron 4-component eigenstate $|\psi_m\rangle$.

For a fixed interatomic distance, R, the Dirac Hamiltonian can be expressed as follows:

$$H = c\,\boldsymbol{\alpha}\cdot\mathbf{p} + \beta\,c^2 + V_{\rm TC}, \tag{4}$$

where $\mathbf{p} = -i\hbar\boldsymbol{\nabla}$ is the electron momentum operator, c is the speed of light and the Dirac matrices, $\boldsymbol{\alpha} = (\alpha_x, \alpha_y, \alpha_z)$ and β, are given by

$$\alpha_\xi = \begin{pmatrix} 0 & \sigma_\xi \\ \sigma_\xi & 0 \end{pmatrix};\ \text{and}\ \beta = \begin{pmatrix} I & 0 \\ 0 & -I \end{pmatrix}, \tag{5}$$

with

$$\sigma_x = \begin{pmatrix} 0 & 1 \\ 1 & 0 \end{pmatrix};\ \sigma_y = \begin{pmatrix} 0 & -i \\ i & 0 \end{pmatrix};\ \text{and}\ \sigma_z = \begin{pmatrix} 1 & 0 \\ 0 & -1 \end{pmatrix},$$

where the set of σ_ξ is composed by the Pauli matrices and I is a 2×2 unitary matrix [49]. The molecular orbitals are 4-component vectors given by $\langle\mathbf{r}|\psi_m\rangle = (\psi_1, \psi_2, \bar{\psi}_3, \bar{\psi}_4)$, where the first two components form what is known as the large component, while the last two are referred to as the small component of a relativistic wavefunction. Consequently, the two-center Dirac equation can be expanded in terms of these four components, yielding the following expression:

$$c\,p_z\bar{\psi}_3 + c(p_x - ip_y)\bar{\psi}_4 + V_{\rm TC}\psi_1 + (mc^2 - E)\psi_1 = 0; \tag{6a}$$

$$-c\,p_z\bar{\psi}_4 + c(p_x + ip_y)\bar{\psi}_3 + V_{\rm TC}\psi_2 + (mc^2 - E)\psi_2 = 0; \tag{6b}$$

$$c\,p_z\psi_1 + c(p_x - ip_y)\psi_2 + V_{\rm TC}\bar{\psi}_3 - (mc^2 + E)\bar{\psi}_3 = 0; \tag{6c}$$

$$-c\,p_z\psi_2 + c(p_x + ip_y)\psi_1 + V_{\rm TC}\bar{\psi}_4 - (mc^2 + E)\bar{\psi}_4 = 0. \tag{6d}$$

From Eq.(6), one clearly sees that the two-center Coulomb potential is diagonal in terms of large and small components. It does not mix the different components. On the contrary, the kinetic energy part of the Dirac Hamiltonian, composed by the $\boldsymbol{\alpha}$ matrix, mixes the small and the large components of the wave function. As we will see, we are then forced to compute matrix elements involving a the combination of the large and small components. In the following section we present the Dirac operators in Prolate Spheroidal coordinates.

A. Prolate Spheroidal coordinates

A system of coordinates that takes into account the singularities originated by the two-center Coulomb potential is the so-called system of Prolate Spheroidal coordinates (ξ, η, φ), *see* e.g. ref. [47]. The coordinates of the system are defined as follows:

$$\xi = \frac{r_A + r_B}{2a}, \quad \text{for}\ 1 \le \xi < \infty; \tag{7a}$$

$$\eta = \frac{r_A - r_B}{2a}, \quad \text{for}\ -1 \le \eta \le 1; \tag{7b}$$

$$\varphi = \arctan\left(\frac{y}{x}\right), \quad \text{for}\ 0 \le \varphi \le 2\pi. \tag{7c}$$

In Figure 1, a graphical representation of the two-center Coulomb problem is given in the Prolate Spheroidal coordinates.

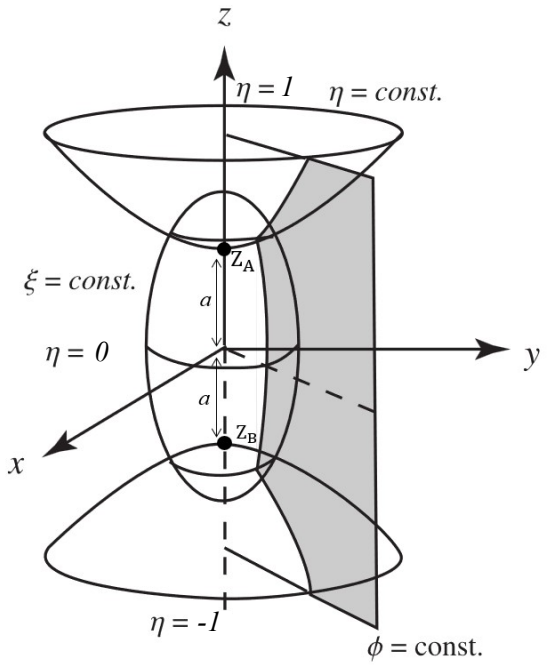

Figure 1. The two-center Coulomb problem in Cartesian and Prolate Spheroidal coordinates where $a = R/2$, R being the interatomic distance between nuclei Z_A and Z_B.

The electron position with respect to the two foci (A and B), given by Eq. (1a) and Eq. (1b), respectively, can be rewritten in Prolate Spheroidal coordinates as

$$r_A = a(\xi + \eta); \tag{8a}$$
$$r_B = a(\xi - \eta), \tag{8b}$$

where the product $r_A r_B$ is given by $a^2(\xi^2 - \eta^2)$. Moreover, the relation between Cartesian and Prolate Spheroidal coordinates is given by the following expressions:

$$x = a\sqrt{(\xi^2-1)(1-\eta^2)}\cos\varphi, \tag{9a}$$
$$y = a\sqrt{(\xi^2-1)(1-\eta^2)}\sin\varphi, \tag{9b}$$
$$z = a\,\xi\,\eta. \tag{9c}$$

Finally, the two-center Coulomb potential, Eq.(2), can be expressed in Prolate Spheroidal coordinates as follows

$$V_{\rm TC}(r_A, r_B) = -\frac{1}{a}\frac{(Z_A+Z_B)\xi + (Z_B - Z_A)\eta}{(\xi^2-\eta^2)}. \tag{10}$$

The linear momentum operators in Eq.(6) are expressed in Prolate Spheroidal coordinates via the first-order derivatives of x, y and z as follows:

$$\frac{\partial}{\partial x} = \frac{1}{a}\frac{\sqrt{(\xi^2-1)(1-\eta^2)}}{(\xi^2-\eta^2)}\xi\cos\varphi\frac{\partial}{\partial\xi} - \frac{1}{a}\frac{\sqrt{(\xi^2-1)(1-\eta^2)}}{(\xi^2-\eta^2)}\eta\cos\varphi\frac{\partial}{\partial\eta} - \frac{1}{a}\frac{\sin\varphi}{\sqrt{(\xi^2-1)(1-\eta^2)}}\frac{\partial}{\partial\varphi}. \tag{11a}$$

$$\frac{\partial}{\partial y} = \frac{1}{a}\frac{\sqrt{(\xi^2-1)(1-\eta^2)}}{(\xi^2-\eta^2)}\xi\sin\varphi\frac{\partial}{\partial\xi} - \frac{1}{a}\frac{\sqrt{(\xi^2-1)(1-\eta^2)}}{(\xi^2-\eta^2)}\eta\sin\varphi\frac{\partial}{\partial\eta} + \frac{1}{a}\frac{\cos\varphi}{\sqrt{(\xi^2-1)(1-\eta^2)}}\frac{\partial}{\partial\varphi}. \tag{11b}$$

$$\frac{\partial}{\partial z} = \frac{1}{a}\frac{(\xi^2-1)}{(\xi^2-\eta^2)}\eta\frac{\partial}{\partial\xi} + \frac{1}{a}\frac{(1-\eta^2)}{(\xi^2-\eta^2)}\xi\frac{\partial}{\partial\eta}. \tag{11c}$$

Additionally, another important operator in Eq.(6) is composed by the combination of the x- and y-components of the linear momentum operator, i.e. $(p_x \pm ip_y)$. This combination is given by the following expression:

$$\frac{\partial}{\partial x} \pm i\frac{\partial}{\partial y} = \frac{1}{a}\frac{e^{\pm i\varphi}}{(\xi^2-\eta^2)}\left[\sqrt{(\xi^2-1)(1-\eta^2)}\left(\xi\frac{\partial}{\partial\xi} - \eta\frac{\partial}{\partial\eta}\right) \pm i\frac{(\xi^2-\eta^2)}{\sqrt{(\xi^2-1)(1-\eta^2)}}\frac{\partial}{\partial\varphi}\right]$$
$$= \frac{1}{a}\frac{\sqrt{(\xi^2-1)(1-\eta^2)}}{(\xi^2-\eta^2)}e^{\pm i\varphi}\left(\xi\frac{\partial}{\partial\xi} - \eta\frac{\partial}{\partial\eta} \pm i\left[\frac{1}{(\xi^2-1)} + \frac{1}{(1-\eta^2)}\right]\frac{\partial}{\partial\varphi}\right). \tag{12a}$$

Finally, the volume element is given by

$$dV = a^3(\xi^2-\eta^2)d\xi d\eta d\varphi. \tag{13}$$

These expressions can be easily compared to the ones accessible in the literature, *see* e.g. ref. [47].

B. Polynomial expansion of the wave function

In Eq. (6), the wave function components $(\psi_1, \psi_2, \bar{\psi}_3, \bar{\psi}_4)$ are divided into two separated sets. On one side, we have the so-called *"large components"*, $|\psi_n\rangle$, for $n = 1$ and $n = 2$. On the other side, the so-called *"small compo-*

nents", $|\bar{\psi}_n\rangle$, for $n = 3$ and $n = 4$. This nomenclature is used here as a reminiscence of the one-center Coulomb problem [50]. Note that this nomenclature is not strictly correct, as the present two-center Coulomb problem does not present spherical symmetry. Nevertheless, this labeling is still useful in order to organize equations and may help the reader to follow our derivations. To sum up, in order to solve Eq. (6), each wave function component, $|\psi_n\rangle$ or $|\bar{\psi}_n\rangle$, can be expanded in terms of a basis set composed by a set of "radial" polynomials and spherical harmonics. In principle, this expansion is exact, however, in practice, the number of radial functions and spherical harmonics is limited to a finite number. As usual, the truncation of this expansion must be based on the quality of the results, and thus, convergence studies are required. Nonetheless, as the basis set used here is defined in Prolate Spheroidal coordinates, one expects a fast and efficient convergence with respect the dimension of the basis [46]. As a result, the large components, $n = 1$ and $n = 2$, are expanded as follows,

$$\begin{aligned}\langle \mathbf{r}|\psi_n\rangle &= \sum_{l=0}^{L_{\max}} R_n^{l,M_n}(\xi) Y_{l_n}^{M_n}(\eta,\phi) \\ &= \sum_{l=0}^{L_{\max}} \sum_{i=1}^{\Omega_n} c_i^l (\xi^2-1)^{|M_n|/2} B_{i_n}^{k_n}(\xi) Y_{l_n}^{M_n}(\eta,\phi) \\ &= \sum_{\mu_n=1}^{\Omega_n\times(L_{\max}+1)} c_{\mu_n}|\chi_{\mu_n}\rangle, \end{aligned} \tag{14}$$

where $\{c_{\mu_n}\} \equiv \{c_i^l\}$ and the index "μ_n" gathers the indices "l" and "i". The dimension of the basis is then given by the total number of radial polynomial functions, Ω_n, and the maximum number of spherical harmonics used in the expansion, $L_{\max}+1$. In Prolate Spheroidal coordinates, the basis function is represented as follows,

$$\langle \mathbf{r}|\chi_{\mu_n}\rangle = (\xi^2-1)^{|M_n|/2} B_{i_n}^{k_n}(\xi) Y_{l_n}^{M_n}(\eta,\phi). \tag{15}$$

In the same way, the small components of the wave function, $n = 3$ and $n = 4$, are expanded as follows,

$$\begin{aligned}\langle \mathbf{r}|\bar{\psi}_n\rangle &= \sum_{l=0}^{L_{\max}} \bar{R}_n^{l,M_n}(\xi) Y_{l_n}^{M_n}(\eta,\phi) \\ &= \sum_{l=0}^{L_{\max}} \sum_{i=1}^{\Omega_n} i\, c_i^l (\xi^2-1)^{|M_n|/2} B_{i_n}^{k_n}(\xi) Y_{l_n}^{M_n}(\eta,\phi) \\ &= \sum_{\mu_n=1}^{\Omega_n\times(L_{\max}+1)} c_{\mu_n}|\bar{\chi}_{\mu_n}\rangle, \end{aligned} \tag{16}$$

where the basis set function is defined as

$$\langle \mathbf{r}|\bar{\chi}_{\mu_n}\rangle = i\,(\xi^2-1)^{|M_n|/2} B_{i_n}^{k_n}(\xi) Y_{l_n}^{M_n}(\eta,\phi). \tag{17}$$

Note that here k_n indicates the order of the radial polynomial functions and M_n is given by

$$M_1 = M_3 = m - 1/2; \tag{18}$$
$$M_2 = M_4 = m + 1/2. \tag{19}$$

The utilization of this basis transforms the differential equation Eq. (6) into a generalized eigenvalue problem as follows,

$$\begin{pmatrix} \mathbf{V}_{\mathrm{TC}}^{11} & 0 & \mathbf{P}_z^{13} & \mathbf{P}_{(x-iy)}^{14} \\ 0 & \mathbf{V}_{\mathrm{TC}}^{22} & \mathbf{P}_{(x+iy)}^{23} & -\mathbf{P}_z^{24} \\ \mathbf{P}_z^{31} & \mathbf{P}_{(x-iy)}^{32} & \mathbf{V}_{\mathrm{TC}}^{33} & 0 \\ \mathbf{P}_{(x+iy)}^{41} & -\mathbf{P}_z^{42} & 0 & \mathbf{V}_{\mathrm{TC}}^{44} \end{pmatrix} \begin{pmatrix} \mathbf{C}^1 \\ \mathbf{C}^2 \\ \bar{\mathbf{C}}^3 \\ \bar{\mathbf{C}}^4 \end{pmatrix} = E \begin{pmatrix} \mathbf{S}^{11} & 0 & 0 & 0 \\ 0 & \mathbf{S}^{22} & 0 & 0 \\ 0 & 0 & -\mathbf{S}^{33} & 0 \\ 0 & 0 & 0 & -\mathbf{S}^{44} \end{pmatrix} \begin{pmatrix} \mathbf{C}^1 \\ \mathbf{C}^2 \\ \bar{\mathbf{C}}^3 \\ \bar{\mathbf{C}}^4 \end{pmatrix} \tag{20}$$

where the dimension of each matrix is given by the dimension of the basis set. Finally, note that the resulting matrices are composed by the application of the Dirac operators in Eq.(6) onto the basis set functions given by Eq.(15) and Eq.(17). A detailed derivation of the application of the Dirac operators on this basis is given in Appendix A. The computation of the different matrix elements in Eq.(20) is presented in details in the next section.

III. COMPUTATIONAL DETAILS

In this section, we discuss the resolution of Eq.(20). Firstly, we present the complete expression of the matrix elements involved in Eq.(20). Secondly, we propose a numerical resolution of Eq.(20) using the so-called "B-spline Galerkin" method. This approach has been used already in the context of relativistic atomic calculations [8, 51] and, more recently, in the context of relativistic molecular photoionization [4].

A. Expansion of the matrix elements

The matrix elements in Eq. (20) are composed by "radial" integrals times some angular coefficients. The radial integrals involve different radial polynomials and can be computed numerically. The numerical integration of such radial integrals is presented in Section III B. On the con-

trary, the angular coefficients can be derived analytically. These angular coefficients are composed by angular integrals involving different spherical harmonics. In order to compute such angular integrals, different recurrence relations have been derived. The computation of these angular coefficients is the main result of the present work and is presented in Section IV. We pass now to give the complete expressions for each matrix element in Eq.(20). Note that the following notation has been used,

$$\mu_n \equiv \{i_n, l_n\}; \;\; \mu'_n \equiv \{j_n, l'_n\}, \tag{21}$$

where "n" indicates the corresponding wave function component. In addition, note below that the complex conjugation of the radial polynomials has been omitted due to its real character. Here the list of matrix elements:

Elements of the overlap matrix:

$$\mathbf{S}^{nn}(\mu'_n, \mu_n) \equiv \langle \chi_{\mu'_n} | \chi_{\mu_n} \rangle = a^2 \left[\int_1^\infty (\xi^2 - 1)^{M_n} B_{j_n}^{k_n} B_{i_n}^{k_n} d\xi \right] \langle Y_{l'_n}^{M_n} | Y_{l_n}^{M_n} \rangle \,. \tag{22}$$

Elements of the two-center potential matrix:

$$\begin{aligned} \mathbf{V}_{\mathrm{TC}}^{nn}(\mu'_n, \mu_n) \equiv \langle \chi_{\mu'_n} | V_{\mathrm{TC}} | \chi_{\mu_n} \rangle &= a^2 \left[(Z_1 + Z_2) \int_1^\infty \xi (\xi^2 - 1)^{M_n} B_{j_n}^{k_n} B_{i_n}^{k_n} d\xi \right] \langle Y_{l'_n}^{M_n} | Y_{l_n}^{M_n} \rangle \\ &+ a^2 \left[(Z_2 - Z_1) \int_1^\infty \xi (\xi^2 - 1)^{M_n} B_{j_n}^{k_n} B_{i_n}^{k_n} d\xi \right] \langle Y_{l'_n}^{M_n} | Y_{l_n}^{M_n} \rangle \,. \end{aligned} \tag{23}$$

Elements of the z-component of the linear momentum matrix:

$$\begin{aligned} \mathbf{P}_z^{13}(\mu'_1, \mu_3) \equiv \langle \chi_{\mu'_1} | p_z | \chi_{\mu_3} \rangle &= a^2 \left[M_3 \int_1^\infty \xi (\xi^2 - 1)^{\frac{M_3 + M_1}{2}} B_{j_1}^{k_1} B_{i_3}^{k_3} d\xi \right] \langle Y_{l'_1}^{M_1} | \eta | Y_{l_3}^{M_3} \rangle \\ &+ a^2 \left[\int_1^\infty (\xi^2 - 1)^{\frac{M_1 + M_3}{2} + 1} B_{j_1}^{k_1} \frac{\partial}{\partial \xi} B_{i_3}^{k_3} d\xi \right] \langle Y_{l'_1}^{M_1} | \eta | Y_{l_3}^{M_3} \rangle \\ &+ a^2 \left[\int_1^\infty \xi (\xi^2 - 1)^{\frac{M_3 + M_1}{2}} B_{j_1}^{k_1} B_{i_3}^{k_3} d\xi \right] \langle Y_{l'_1}^{M_1} | (1 - \eta^2) \frac{\partial}{\partial \eta} | Y_{l_3}^{M_3} \rangle, \end{aligned} \tag{24}$$

$$\begin{aligned} \mathbf{P}_z^{24}(\mu'_2, \mu_4) \equiv \langle \chi_{\mu'_2} | p_z | \chi_{\mu_4} \rangle &= a^2 \left[M_4 \int_1^\infty \xi (\xi^2 - 1)^{\frac{M_2 + M_4}{2}} B_{j_2}^{k_2} B_{i_4}^{k_4} d\xi \right] \langle Y_{l'_2}^{M_2} | \eta | Y_{l_4}^{M_4} \rangle \\ &+ a^2 \left[\int_1^\infty (\xi^2 - 1)^{\frac{M_2 + M_4}{2} + 1} B_{j_2}^{k_2} \frac{\partial}{\partial \xi} B_{i_4}^{k_4} d\xi \right] \langle Y_{l'_2}^{M_2} | \eta | Y_{l_4}^{M_4} \rangle \\ &+ a^2 \left[\int_1^\infty \xi (\xi^2 - 1)^{\frac{M_2 + M_4}{2}} B_{j_2}^{k_2} B_{i_4}^{k_4} d\xi \right] \langle Y_{l'_2}^{M_2} | (1 - \eta^2) \frac{\partial}{\partial \eta} | Y_{l_4}^{M_4} \rangle, \end{aligned} \tag{25}$$

$$\begin{aligned} \mathbf{P}_z^{31}(\mu'_3, \mu_1) \equiv \langle \chi_{\mu'_3} | p_z | \chi_{\mu_1} \rangle &= a^2 \left[M_1 \int_1^\infty \xi (\xi^2 - 1)^{\frac{M_1 + M_3}{2}} B_{j_3}^{k_3} B_{i_1}^{k_1} d\xi \right] \langle Y_{l'_3}^{M_3} | \eta | Y_{l_1}^{M_1} \rangle \\ &+ a^2 \left[\int_1^\infty (\xi^2 - 1)^{\frac{M_3 + M_1}{2} + 1} B_{j_3}^{k_3} \frac{\partial}{\partial \xi} B_{i_1}^{k_1} d\xi \right] \langle Y_{l'_3}^{M_3} | \eta | Y_{l_1}^{M_1} \rangle \\ &+ a^2 \left[\int_1^\infty \xi (\xi^2 - 1)^{\frac{M_1 + M_3}{2}} B_{j_3}^{k_3} B_{i_1}^{k_1} d\xi \right] \langle Y_{l'_3}^{M_3} | (1 - \eta^2) \frac{\partial}{\partial \eta} | Y_{l_1}^{M_1} \rangle, \end{aligned} \tag{26}$$

$$\begin{aligned} \mathbf{P}_z^{42}(\mu'_4, \mu_2) \equiv \langle \chi_{\mu'_4} | p_z | \chi_{\mu_2} \rangle \;\; &= a^2 \left[M_2 \int_1^\infty \xi (\xi^2 - 1)^{\frac{M_2 + M_4}{2}} B_{j_4}^{k_4} B_{i_2}^{k_2} d\xi \right] \langle Y_{l'_4}^{M_4} | \eta | Y_{l_2}^{M_2} \rangle \\ &+ a^2 \left[\int_1^\infty (\xi^2 - 1)^{\frac{M_4 + M_2}{2} + 1} B_{j_4}^{k_4} \frac{\partial}{\partial \xi} B_{i_2}^{k_2} d\xi \right] \langle Y_{l'_4}^{M_4} | \eta | Y_{l_2}^{M_2} \rangle \\ &+ a^2 \left[\int_1^\infty \xi (\xi^2 - 1)^{\frac{M_2 + M_4}{2}} B_{j_4}^{k_4} B_{i_2}^{k_2} d\xi \right] \langle Y_{l'_4}^{M_4} | (1 - \eta^2) \frac{\partial}{\partial \eta} | Y_{l_2}^{M_2} \rangle. \end{aligned} \tag{27}$$

Elements of the $(x \pm iy)$-components of the linear momentum matrix:

$$\mathbf{P}_{(x-iy)}^{14}(\mu'_1, \mu_4) \equiv \langle \chi_{\mu'_1} | p_x - i p_y | \chi_{\mu_4} \rangle = a^2 \left[\int_1^\infty \xi (\xi^2 - 1)^{\frac{M_1 + M_4}{2}} B_{j_1}^{k_1} \frac{\partial}{\partial \xi} B_{i_4}^{k_4} d\xi \right] \langle Y_{l'_1}^{M_1} | (1 - \eta^2)^{1/2} e^{-i\varphi} | Y_{l_4}^{M_4} \rangle$$

$$+ a^2\ 2M_4 \left[\int_1^\infty \xi^2(\xi^2-1)^{\frac{M_1+M_4}{2}-1} B_{j_1}^{k_1} B_{i_4}^{k_4} d\xi\right] \langle Y_{l_1'}^{M_1}|(1-\eta^2)^{1/2} e^{-i\varphi}|Y_{l_4}^{M_4}\rangle$$
$$- a^2 \left[\int_1^\infty (\xi^2-1)^{\frac{M_1+M_4}{2}+1} B_{j_1}^{k_1} B_{i_4}^{k_4} d\xi\right] \langle Y_{l_n'}^{M_1}|\eta\,(1-\eta^2)^{1/2} \frac{\partial}{\partial\eta} e^{-i\varphi}|Y_{l_n}^{M_4}\rangle$$
$$+ a^2\ M_4 \left[\int_1^\infty (\xi^2-1)^{\frac{M_1+M_4}{2}+1} B_{j_1}^{k_1} B_{i_4}^{k_4} d\xi\right] \langle Y_{l_n'}^{M_1}|\frac{\eta^2}{(1-\eta^2)^{1/2}} e^{-i\varphi}|Y_{l_n}^{M_4}\rangle, \quad (28)$$

$$\mathbf{P}^{23}_{(x+iy)}(\mu_2',\mu_3) \equiv \langle\chi_{\mu_2'}|p_x+ip_y|\chi_{\mu_3}\rangle = a^2 \left[\int_1^\infty \xi(\xi^2-1)^{\frac{M_2+M_3}{2}+1} B_{j_2}^{k_2} \frac{\partial}{\partial\xi} B_{i_3}^{k_3} d\xi\right] \langle Y_{l_2'}^{M_2}|(1-\eta^2)^{1/2} e^{i\varphi}|Y_{l_3}^{M_3}\rangle$$
$$- a^2 \left[\int_1^\infty (\xi^2-1)^{\frac{M_2+M_3}{2}+1} B_{j_2}^{k_2} B_{i_3}^{k_3} d\xi\right] \langle Y_{l_2}^{M_2}|\eta\,(1-\eta^2)^{1/2} \frac{\partial}{\partial\eta} e^{i\varphi}|Y_{l_3}^{M_3}\rangle$$
$$- a^2 M_3 \left[\int_1^\infty (\xi^2-1)^{\frac{M_2+M_3}{2}+1} B_{j_2}^{k_2} B_{i_3}^{k_3} d\xi\right] \langle Y_{l_2'}^{M_2}|\frac{\eta^2}{(1-\eta^2)^{1/2}} e^{i\varphi}|Y_{l_3}^{M_3}\rangle \quad (29)$$

$$\mathbf{P}^{32}_{(x-iy)}(\mu_3',\mu_2) \equiv \langle\chi_{\mu_3'}|p_x-ip_y|\chi_{\mu_2}\rangle = a^2 \left[\int_1^\infty \xi(\xi^2-1)^{\frac{M_3+M_2}{2}} B_{j_3}^{k_3} \frac{\partial}{\partial\xi} B_{i_2}^{l,k_2} d\xi\right] \langle Y_{l_3'}^{M_3}|(1-\eta^2)^{1/2} e^{-i\varphi}|Y_{l_2}^{M_2}\rangle$$
$$+ a^2\ 2M_2 \left[\int_1^\infty \xi^2(\xi^2-1)^{\frac{M_3+M_2}{2}-1} B_{j_3}^{k_3} B_{i_2}^{k_2} d\xi\right] \langle Y_{l_3'}^{M_3}|(1-\eta^2)^{1/2} e^{-i\varphi}|Y_{l_2}^{M_2}\rangle$$
$$- a^2 \left[\int_1^\infty (\xi^2-1)^{\frac{M_3+M_2}{2}+1} B_{j_3}^{k_3} B_{i_2}^{k_2} d\xi\right] \langle Y_{l_3'}^{M_3}|\eta\,(1-\eta^2)^{1/2} \frac{\partial}{\partial\eta} e^{-i\varphi}|Y_{l_2}^{M_2}\rangle$$
$$+ a^2\ M_2 \left[\int_1^\infty (\xi^2-1)^{\frac{M_3+M_2}{2}+1} B_{j_3}^{k_3} B_{i_2}^{k_2} d\xi\right] \langle Y_{l_3'}^{M_3}|\frac{\eta^2}{(1-\eta^2)^{1/2}} e^{-i\varphi}|Y_{l_2}^{M_2}\rangle, \quad (30)$$

$$\mathbf{P}^{41}_{(x+iy)}(\mu_4',\mu_1) \equiv \langle\chi_{\mu_4'}|p_x+ip_y|\chi_{\mu_1}\rangle = a^2 \left[\int_1^\infty \xi(\xi^2-1)^{\frac{M_4+M_1}{2}+1} B_{j_4}^{k_4} \frac{\partial}{\partial\xi} B_{i_1}^{k_1} d\xi\right] \langle Y_{l_4'}^{M_4}|(1-\eta^2)^{1/2} e^{i\varphi}|Y_{l_1}^{M_1}\rangle$$
$$- a^2 \left[\int_1^\infty (\xi^2-1)^{\frac{M_4+M_1}{2}+1} B_{j_4}^{k_4} B_{i_1}^{k_1} d\xi\right] \langle Y_{l_4'}^{M_4}|\eta\,(1-\eta^2)^{1/2} \frac{\partial}{\partial\eta} e^{i\varphi}|Y_{l_1}^{M_1}\rangle$$
$$- a^2\ M_1 \left[\int_1^\infty (\xi^2-1)^{\frac{M_4+M_1}{2}+1} B_{j_4}^{k_4} B_{i_1}^{k_1} d\xi\right] \langle Y_{l_4'}^{M_4}|\frac{\eta^2}{(1-\eta^2)^{1/2}} e^{i\varphi}|Y_{l_1}^{M_1}\rangle. \quad (31)$$

B. Numerical implementation

In order to solve Eq.(20), one can follow the so-called B-spline Galerkin method implemented in ref. [4]. As we have introduced in Section II B, the large and the small components of the wave function are expanded in terms of different polynomial basis sets. These polynomials are given here by B-splines. B-splines are piecewise polynomial functions (L^2-integrable functions defined in a restricted sampled space) which have smooth connection between different pieces. As a result, B-splines are very flexible, allowing us to fit any kind of continuous curve. In fact, the term "spline" makes reference to old industrial designers who, in the past, used to draw continuous and smooth curves over a sequence of "knot points" with the help of a piece of rubber named spline. The B-splines were formally introduced by Schoenberg [52] and popularized by de Boor's work [53]. In atomic and molecular physics, B-splines have demonstrated their ability to solve bound state and scattering problems, *see* ref. [46]. Today, B-splines are recognized as a powerful tool when continuum solutions are required. The success of these functions is directly related to their effective "completeness", i.e. their capacity to approach L^2 completeness without numerical instabilities [54]. The application of B-splines to relativistic atomic problems was discussed in details by Froese-Fischer and Zatsarinny [8]. These authors proposed, for the first time, the utilization of two different B-spline basis: one for the large component and a second one for the small component. This strategy imposes the correct boundary conditions. As a consequence, the so-called *"spurious states"* are avoided [8]. This strategy has been recently implemented by Zapata *et al.* in ref. [4] to solve the two-center Dirac equation within the one-center-expansion approximation in Spherical coordinates, showing the possibility of using the B-spline Galerkin method in the context of relativistic molecular calculations. In this regard, we do not expect any problem in the implementation of the B-spline Galerkin method to solve the present problem.

As we propose in Section II B, the different components of the wave function are expanded in different B-splines basis (referred here as 'radial polynomials"). Following ref. [4] and ref. [8], the utilization of different B-spline orders ensures the application of the correct boundary conditions to the problem. Then, we define each B-spline basis over different sequences of increasing knot points where the boundary knots are chosen to be k_n-

fold degenerate, e.g. $r_1 = r_2 = ... = r_{k_n} = r_{\min}$ and $r_{\Omega_n+1} = r_{\Omega_n+2} = ... = r_{\Omega_n+k_n} = r_{\max}$, where k_n is the order of the B-splines and Ω_n the number of B-splines for each basis set, *see* Eq.(14) and Eq.(16). For bound state calculations, we applied the so-called "zero boundary conditions" at $r = r_{\min}$ and $r = r_{\max}$ by removing the first and last B-spline from the basis sets. The resulting B-spline integrals, in this work referred as "radial integrals", can be computed to machine accuracy using Gauss-Legendre's quadrature [55]. The angular coefficients that multiply the radial integrals in Eq.(20) are computed analytical and are given in Section IV.

The computation of the continuum states can be computed following the prescriptions given in ref. [4]. To summarize, the matrix $\mathbf{W}(E) = \mathbf{H} - E\mathbf{S}$ is diagonalized at each continuum energy E, using an inverse iteration procedure to extract the independent continuum solutions [44, 45]. The resulting solutions are obtained with arbitrary normalization and phase. Therefore, the last step consists on imposing the correct norm and asymptotic behavior. To do so, the numerical solution is fitted to a linear combination of asymptotic regular and irregular Dirac-Coulomb waves [4], allowing us to reconstruct the K- and S-matrices. The diagonalization of the K-matrix results in the partial-wave phase shifts, from where information about the molecular potential and scattering events can be extracted. Finally, the correct solution is obtained by multiplying the numerical solution by the corresponding S-matrix. See more details about this procedure in ref. [4].

The present numerical method can be implemented only if the angular coefficients in Eq.(20) are computed analytically. To the best of our knowledge, the computation of these angular coefficients cannot be found in the literature. For this reason, we present here a full derivation and computation of the angular coefficients involving different spherical harmonics, *see* Eq.(22)-(31).

IV. RESULTS AND DISCUSSION

In this section, we present the derivation and computation of the angular coefficients given in Eq.(22)-(31). These angular coefficients are angular integrals involving different spherical harmonics and some angular operators. In order to solve such angular integrals, we make use of the properties of the spherical harmonics, *see* ref. [56] and ref. [57]. In this work, the spherical harmonics are defined as follows,

$$Y_l^m(\eta, \varphi) = P_l^m(\eta)\, e^{im\varphi}, \tag{32}$$

where $P_l^m(\eta)$ stands for the so-called normalized associated Legendre polynomials [56]. In addition, the so-called Condon-Shortley phase convention is used here, i.e.

$$Y_l^{-m} = (-1)^m (Y_l^m)^*. \tag{33}$$

Note that the spherical harmonics form an orthonormal basis, so one can easily verify the following condition:

$$\int_{-1}^{1}\int_{0}^{2\pi} (Y_k^n)^*\, Y_l^m d\eta\, d\varphi = \delta_{k,l}\, \delta_{n,m}. \tag{34}$$

Finally, we have to mention that the recurrence relations of the spherical harmonics are directly related to the recurrence relations of the associated Legendre polynomials, *see* Eq.(32). For this reason, the present Section is divided as follows.

In Section IV A, we summarize the recurrence relations of the associated Legendre polynomials required to compute the angular coefficients given in Eq.(22)-(31). In addition, we derive some extra recurrence relations that, to the best of our knowledge, cannot be found in the literature. Then, the validity of these recurrence relations is checked numerically for a series of cases. Finally, in Section IV B, we compute the angular integrals involved in Eq.(22)-(31).

A. Recurrence relations

Legendre's differential equation poses two solutions: the associated Legendre polynomials of the first kind, $\tilde{P}_l^m(\eta)$ and the associated Legendre polynomials of the second kind, $\tilde{Q}_l^m(\eta)$ [57]. For real values of η in the interval $\eta \in [-1, 1]$, the associated Legendre polynomials of the first kind are given by

$$\tilde{P}_l^m(\eta) = \frac{(1-\eta^2)^{m/2}}{2^l l!} \frac{d^{l+m}}{d\eta^{l+m}} (\eta^2 - 1)^l. \tag{35}$$

On the contrary, the associated Legendre polynomials of the second kind diverge for $\eta \in [-1, 1]$. Our attention is then focused now on the associated Legendre polynomials of the first kind, $\tilde{P}_l^m(\eta)$.

We can define now the so-called normalized associated Legendre polynomials, given by the following product, $P_l^m(\eta) = N\tilde{P}_l^m(\eta)$, where the normalization factor N is given by

$$N = \left[\frac{(2l+1)(l-m)!}{4\pi(l+m)!}\right]^{1/2}. \tag{36}$$

Considering this normalization factor, the orthogonality relation of the normalized associated Legendre polynomials is given by the following expression:

$$\int_{-1}^{1} P_k^m\, P_l^m d\eta = (2\pi)^{-1}\delta_{k,l}. \tag{37}$$

Some important derivatives of the associated Legendre polynomials are listed below:

$$(1-\eta^2)^{1/2}\frac{d}{d\eta}\tilde{P}_l^m = \frac{1}{2}\left[\tilde{P}_l^{m+1} - (l+m)(l-m+1)\tilde{P}_l^{m-1}\right]. \quad (38)$$

$$\eta(1-\eta^2)^{1/2}\frac{d}{d\eta}\tilde{P}_l^m = \frac{1}{2}\frac{(l+m+1)}{(2l+1)}\tilde{P}_{l-1}^{m+1} + \frac{1}{2}\frac{(l-m)}{(2l+1)}\tilde{P}_{l+1}^{m+1} - \frac{1}{2}\frac{(l+m)(l-m+1)(l+m-1)}{(2l+1)}\tilde{P}_{l-1}^{m-1} - \frac{1}{2}\frac{(l+m)(\ell-m+1)(l-m+2)}{(2l+1)}\tilde{P}_{l+1}^{m-1}. \quad (39)$$

$$(1-\eta^2)\frac{d}{d\eta}\tilde{P}_l^m = (1-\eta^2)^{1/2}\tilde{P}_l^{m+1} - m\,\eta\,\tilde{P}_l^m = \frac{(l+m)(l+1)}{(2l+1)}\tilde{P}_{l-1}^m - \frac{l(l-m+1)}{(2l+1)}\tilde{P}_{l+1}^m. \quad (40)$$

We pass now to list the recurrence relations needed for the analytical evaluation of the angular integrals given in Eq.(22)-(31).

1. First recurrence relation

The first recurrence relation is defined in Eq.(2.5.20) in ref. [56] and is given by the following expression:

$$\eta\tilde{P}_l^m = \frac{(l-m+1)}{(2l+1)}\tilde{P}_{l+1}^m + \frac{(l+m)}{(2l+1)}\tilde{P}_{l-1}^m. \quad (41)$$

2. Second recurrence relation

Our second recurrence relation is given by the following expression:

$$(1-\eta^2)^{1/2}\tilde{P}_l^m = \left[\frac{(l+m)(l+m-1)}{(2l+1)}\right]\tilde{P}_{l-1}^{m-1} + \left[\frac{(l+m)(l-m+2)-(2l+1)(l+m-2)}{(2l+1)}\right]\tilde{P}_{l+1}^{m-1}. \quad (42)$$

This recurrence relation can be derived from Eq.(2.5.23) and Eq.(2.5.20) in ref. [56] and by changing m to $m-1$.

3. Third recurrence relation

The third recurrence relation is given by the following expression:

$$(1-\eta^2)^{1/2}\tilde{P}_l^{m-1} = \frac{1}{(2l+1)}\left[\tilde{P}_{l+1}^m - \tilde{P}_{l-1}^m\right]. \quad (43)$$

This relation can be derived from the derivative of the common Legendre polynomials, $\tilde{P}_l(\eta)$, and using Eq.(3-41) in ref. [58].The starting point is the recurrence relation for the common Legendre polynomials,

$$(2l+1)\tilde{P}_l = \tilde{P}'_{l+1} - \tilde{P}'_{l-1}. \quad (44)$$

The second step consists on differentiating Eq.(44) "$m-1$"-times as follows

$$(2l+1)\frac{d^{m-1}}{d\eta^{m-1}}\tilde{P}_l = \frac{d^{m-1}}{d\eta^{m-1}}\left[\frac{d}{d\eta}\tilde{P}_{l+1} - \frac{d}{d\eta}\tilde{P}_{l-1}\right]. \quad (45)$$

The final step consists on using the definition of the associated Legendre polynomials of the first kind given by Eq.(35) and we arrive to the following expression:

$$(2l+1)(1-\eta^2)^{1/2}\tilde{P}_l^{m-1} = \tilde{P}_{l+1}^m - \tilde{P}_{l-1}^m, \quad (46)$$

and rearranging the terms we arrive to Eq.(43).

4. Fourth recurrence relation

The fourth recurrence relation is given by the following expression:

$$(1-\eta^2)^{1/2}\tilde{P}_l^{m+1} = (l+m)\tilde{P}_{l-1}^m - (l-m)\eta\tilde{P}_l^m. \quad (47)$$

This recurrence relation can be derived using Eq.(2.5.25) from ref. [56] together with our Eq.(40).

5. Fifth recurrence relation

The fifth recurrence relation is given by the following expression:

$$(1-\eta^2)^{1/2}\tilde{P}_l^m = (l+m-1)\tilde{P}_{l-1}^{m-1} - (l-m+1)\eta\tilde{P}_l^{m-1}. \quad (48)$$

This expression is obtained by changing m to $m-1$ in Eq.(47).

6. Sixth recurrence relation

The sixth recurrence relation is given by the following expression:

$$\frac{\eta^2}{(1-\eta^2)^{1/2}}\tilde{P}_l^m = \frac{(l-m)}{2m(2l+1)}\tilde{P}_{l+1}^{m+1} + \frac{(l+m+1)}{2m(2l+1)}\tilde{P}_{l-1}^{m+1}$$

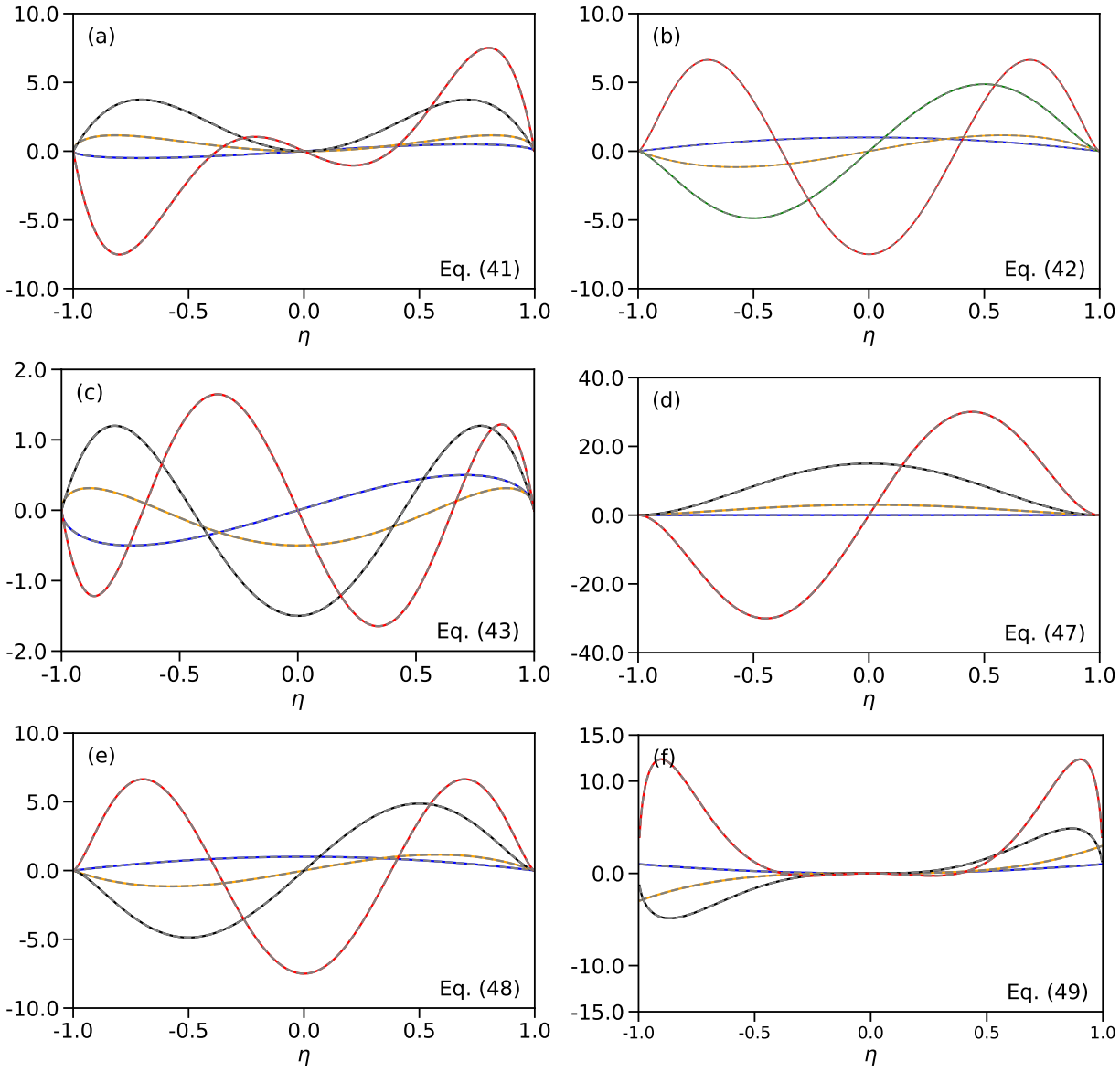

Figure 2. Numerical validation of the recurrence relations derived in this work: Eq. (41), Eq. (42), Eq. (43), Eq. (47), Eq. (48) and Eq. (49). Solid lines correspond to the analytical expressions (right-hand-side of the derived formulas). Dashed (gray) lines correspond to the numerical values obtained using NumPy 2.5.0 library (left-hand-side of the derived formulas). The colors correspond to different l and m cases: $l = 1$ and $m = 1$ (blue); $l = 2$ and $m = 1$ (orange); $l = 3$ and $m = 2$ (black); $l = 4$ and $m = 2$ (red).

$$+\frac{(l+m)(l-m+1)(l-m+2)}{2m(2l+1)}\tilde{P}_{l+1}^{m-1} + \frac{(l+m)(l-m+1)(l+m-1)}{2m(2l+1)}\tilde{P}_{l}^{m-1}. \tag{49}$$

This equation can be derived by multiplying Eq.(2.5.24) in ref. [56] by $(1-\eta^2)^{-1/2}$. Then, one gets the following intermediate step,

$$\frac{\eta}{(1-\eta^2)^{1/2}}\tilde{P}_l^m = \frac{\tilde{P}_l^{m+1}}{2m} + \frac{(l+m)(l-m+1)}{2m}\tilde{P}_l^{m-1}. \tag{50}$$

Finally, we use the first recurrence relation, Eq.(41), and we arrive to Eq.(49).

The validity of the different recurrence relations have been checked numerically. We have performed a systematic numerical test for each recurrence relation by comparing the analytical expression (right-hand-side term of the recurrence relation) with the corresponding numerical value (left-hand-side term of the recurrence relation). The numerical evaluation have been performed using the NumPy 2.5.0 library for different values of η in the range of -1 to 1. In Figure 2, the different recurrence relations are shown for a series of l and m cases.

B. Angular integrals between different spherical harmonics

Once we have derived and validated the required recurrence relations for the associated Legendre polynomials, we can now pass to resolve the angular integrals involving different spherical harmonics appearing in Eq.(22)-(31). As different components of the wave function may be involved in the same angular integral, in order to be consistent with the expressions given in Eq.(22)-(31), the subindex "n" is substituted here by two new subindices, "r" and "s", representing the wave function components involved in the integral.

Finally, note that the first angular integral involved in Eq.(22)-(31) is basically given by the orthogonality relation of the spherical harmonics, given by Eq.(34). The rest of angular integrals are more complex and are composed by angular operators of η. As we can see, the simplicity of the resulting angular coefficients makes the numerical implementation proposed in Section III B totally feasible. We present below the list of angular integrals involved in the resolution of the two-center Dirac equation in Prolate Spheroidal coordinates given by Eq.(22)-(31):

1. First angular integral

The first angular integral is given by the orthogonality condition of the spherical harmonics, Eq.(34). This expression can be re-written as follows:

$$\langle Y_{l'_r}^{M_r}|Y_{l_r}^{M_r}\rangle = \delta_{l'_r,l_r}\delta_{M'_r,M_r}, \tag{51}$$

for $r = 1, 2, 3$ or 4.

2. Second angular integral

The second angular integral is obtained using the first recurrence relation, Eq. (41), and is given by the following expression:

$$\langle Y_{l'_r}^{M_r}|\eta|Y_{l_s}^{M_s}\rangle = \left[\frac{l_s - M_s + 1}{2l_s + 1}\right]\delta_{l'_r,l_s+1} + \left[\frac{l_s + M_s}{2l_s + 1}\right]\delta_{l'_r,l_s-1}, \tag{52}$$

for $r = 1$ and $s = 3$ (or $r = 3$ and $s = 1$), and for $r = 2$ and $s = 4$ (or $r = 4$ and $s = 2$).

3. Third angular integral

The third angular integral is computed using the second recurrence relation, Eq.(42), and is given by the following expression:

$$\langle Y_{l'_r}^{M_r}|(1-\eta^2)^{1/2}e^{-i\varphi}|Y_{l_s}^{M_s}\rangle = \left[\frac{2l_s(m - l_s - 2)}{2l_s + 1}\right]\delta_{l'_r,l_s+1} + \left[\frac{l_s + M_s - 1}{2l_s + 1}\right]\delta_{l'_r,l_s-1}. \tag{53}$$

for $r = 1$ and $s = 4$ (or $r = 3$ and $s = 2$).

4. Forth angular integral

The forth angular integral is computed using the third recurrence relation, Eq. (43), and is given by the following expression:

$$\langle Y_{l'_s}^{M_s}|(1-\eta^2)^{1/2}e^{-i\varphi}|Y_{l_r}^{M_r}\rangle = \frac{1}{2l_r + 1}\left[\delta_{l'_s,l_r+1} - \delta_{l'_s,l_r-1}\right], \tag{54}$$

for $r = 1$ and $s = 4$ (or $r = 3$ and $s = 2$).

5. Fifth and sixth angular integrals

The fifth and sixth angular integrals are composed by a combination of two angular integrals. These integrals are derived using using Eq.(40), Eq. (41) and Eq.(49). The expressions for the fifth and the sixth angular integrals are listed below, respectivley:

$$\left[\langle Y_{l'_r}^{M_r}|e^{-i\varphi}(1-\eta^2)^{1/2}\eta\frac{\partial}{\partial\eta}|Y_{l_s}^{M_s}\rangle - M_s\langle Y_{l'_r}^{M_r}|\frac{e^{-i\varphi}\eta^2}{(1-\eta^2)^{1/2}}|Y_{l_s}^{M_s}\rangle\right] = -\left[\frac{(l_s + M_s)(l_s - M_s + 1)(l_s - M_s + 2)}{(2l_s + 1)}\right]\delta_{l'_r,l_s+1} - \left[\frac{(l_s + M_s)(l_s - M_s + 1)(l_s + M_s - 1)}{(2l_s + 1)}\right]\delta_{l'_r,l_s-1}, \tag{55}$$

$$\left[\langle Y_{l'_s}^{M_s}|e^{-i\varphi}(1-\eta^2)^{1/2}\eta\frac{\partial}{\partial\eta}|Y_{l_r}^{M_r}\rangle + M_r\langle Y_{l'_s}^{M_s}|\frac{e^{-i\varphi}\eta^2}{(1-\eta^2)^{1/2}}|Y_{l_r}^{M_r}\rangle\right] = \left[\frac{(l_r-M_r)}{(2l_r+1)}\right]\delta_{l'_s,l_r+1} + \left[\frac{(l_r+M_r+1)}{(2l_r+1)}\right]\delta_{l'_s,l_r-1}, \tag{56}$$

for $r=1$ and $s=4$, and for $r=3$ and $s=2$.

V. CONCLUSION

In this work, the angular integrals arising from the one-electron two-center Dirac problem have been derived analytically. Prolate Spheroidal coordinates have been implemented and the Dirac operators were explicitly formulated in this coordinate system. The 4-component wave function has been represented in terms of a basis set composed by B-splines and spherical harmonics. The relativistic kinetic-energy and potential-energy operators were derived in this representation, leading to matrix elements that can be separated into radial and angular contributions. As suggested here, the resulting radial integrals can be evaluated numerically using well-established methods such as the B-spline Galerkin method. On the other side, the corresponding angular integrals are treated analytically through the properties of the associated Legendre polynomials. In order to evaluate the angular integrals, we have derived several recurrence relations for the associated Legendre polynomials that cannot be found in the existing literature. As a way to check the validity of the derived recurrence relations, we have performed a systematic numerical test using the library NumPy 2.5.0. An excellent agreement between the numerical evaluation and the analytical expressions was found.

As a result, the angular coefficients provided here can be seen as the analytical "ingredients" required for the construction of the molecular Dirac Hamiltonian. In such a way, the present work contributes to the development of an explicit computational framework for the resolution of the molecular Dirac equation for both bound and continuum states. The results of the present work can be directly used in scattering problems or in relativistic electronic structure calculations. Moreover, the utilization of Prolate Spheroidal coordinates allows one to explore striking scenarios with high accuracy, particularly, in the investigation of core-level photoionization processes in heavy molecules.

VI. AVAILABILITY OF DATA AND MATERIAL

No datasets were generated or analyzed during the current investigation.

VII. ACKNOWLEDGMENTS

This work has been supported by Erasmus Mundus Master's Degree programme in Theoretical Chemistry and Computational Modelling (EM-TCCM) through the European Education and Culture Executive Agency (EACEA) Erasmus Mundus+ scholarship (ref: 101180348), the MSCA H2020 programme (ref: 101034324), the project "Ayudas para la Realización de Proyectos I+D Liderados por Doctores Emergentes" (ref: PR17/24-31945) funded by the Comunidad de Madrid, the project "Ayuda Atracción de Talento César Nombela" (ref: 2025-T1/TEC-36365) funded by the Comunidad de Madrid and the project "Proyectos de Generación de Conocimiento 2025" (ref: PID2025-168755NB-C22) funded by the Agencia Española de Investigación and the Spanish Ministerio de Ciencia, Innovación y Universidades.

Appendix A: The action of the Dirac operators in Prolate Spheroidal coordinates

The application of the different Dirac operators onto the basis set elements, given by Eq. 14 and 16, is detailed in this Appendix. Note that we have redefined the following constant:

$$\bar{a} = \frac{1}{a(\xi^2-\eta^2)}. \tag{A1}$$

In addition, the subindex "n" indicates a specific wave function component, $(\psi_1, \psi_2, \bar{\psi}_3, \bar{\psi}_4)$.

A.1. Application of the p_z operator:

For $n=1$ and $n=2$ components:

$$\begin{aligned} p_z|\chi_{\mu_n}\rangle &= -i\,\bar{a}\left[(\xi^2-1)\frac{\partial}{\partial\xi}\eta + \xi(1-\eta^2)\frac{\partial}{\partial\eta}\right]|\chi_{\mu_n}\rangle \\ &= -i\,\bar{a}\left[\left(|M_n|\xi(\xi^2-1)^{|M_n|/2}B_i^{k_n} + (\xi^2-1)^{|M_n|/2+1}\frac{\partial}{\partial\xi}B_i^{k_n}\right)\right] - i\,\bar{a}\left[\xi\,(\xi^2-1)^{|M_n|/2}B_{i_n}^{k_n}(1-\eta^2)\frac{\partial}{\partial\eta}Y_{l_n}^{M_n}\right]. \end{aligned} \tag{A2}$$

For $n=3$ and $n=4$ components:

$$\begin{aligned} p_z|\chi_{\bar{\mu}_n}\rangle =& -i\,\bar{a}\left[(\xi^2-1)\frac{\partial}{\partial\xi}\eta+\xi(1-\eta^2)\frac{\partial}{\partial\eta}\right]|\chi_{\bar{\mu}_n}\rangle \\ =&\bar{a}\left[\left(|M_n|\xi(\xi^2-1)^{|M_n|/2}B_i^{k_n}+(\xi^2-1)^{|M_n|/2+1}\frac{\partial}{\partial\xi}B_i^{k_n}\right)\right]+\bar{a}\left[\xi\,(\xi^2-1)^{|M_n|/2}B_{i_n}^{k_n}(1-\eta^2)\frac{\partial}{\partial\eta}Y_{l_n}^{M_n}\right]. \end{aligned} \tag{A3}$$

A.2. Application of the $(p_x \pm ip_y)$ operator:
For $n=1$ component:

$$\begin{aligned} (p_x+ip_y)|\chi_{\mu_1}\rangle &= -ie^{i\varphi}\,\bar{a}\left[\sqrt{(\xi^2-1)(1-\eta^2)}\xi\frac{\partial}{\partial\xi}-\sqrt{(\xi^2-1)(1-\eta^2)}\eta\frac{\partial}{\partial\eta}+i\frac{(\xi^2-\eta^2)}{\sqrt{(\xi^2-1)(1-\eta^2)}}\frac{\partial}{\partial\varphi}\right]|\chi_{\mu_1}\rangle \\ &= -i\,\bar{a}\left[(\xi^2-1)^{\frac{M_1+1}{2}}\xi\frac{\partial}{\partial\xi}B_{i_n}^{k_1}e^{i\varphi}(1-\eta^2)^{1/2}Y_{l_n}^{M_1}-(\xi^2-1)^{\frac{M_1+1}{2}}B_{i_n}^{k_1}\right. \\ &\quad\left.\times\left(e^{i\varphi}(1-\eta^2)^{1/2}\eta\frac{\partial}{\partial\eta}+\frac{M_1e^{i\varphi}\eta^2}{(1-\eta^2)^{1/2}}\right)Y_{l_n}^{M_1}\right] \end{aligned} \tag{A4}$$

For $n=2$ component:

$$\begin{aligned} (p_x-ip_y)|\chi_{\mu_2}\rangle &= -ie^{-i\varphi}\,\bar{a}\left[\sqrt{(\xi^2-1)(1-\eta^2)}\xi\frac{\partial}{\partial\xi}-\sqrt{(\xi^2-1)(1-\eta^2)}\eta\frac{\partial}{\partial\eta}-i\frac{(\xi^2-\eta^2)}{\sqrt{(\xi^2-1)(1-\eta^2)}}\frac{\partial}{\partial\varphi}\right]|\chi_{\mu_2}\rangle \\ &= -i\bar{a}\left[\left((\xi^2-1)^{\frac{M_2}{2}}\xi\frac{\partial}{\partial\xi}B_{i_n}^{k_2}+2M_2(\xi^2-1)^{\frac{M_2-1}{2}}\xi^2B_{i_n}^{k_2}\right)\right. \\ &\quad\left.\times\left(e^{i\varphi}(1-\eta^2)^{1/2}\eta\frac{\partial}{\partial\eta}Y_{l_n}^{M_2}-\frac{M_2e^{i\varphi}\eta^2}{(1-\eta^2)^{1/2}}Y_{l_n}^{M_2}\right)\right]. \end{aligned} \tag{A5}$$

For $n=3$ component:

$$\begin{aligned} (p_x+ip_y)|\chi_{\bar{\mu}_3}\rangle &= -ie^{i\varphi}\,\bar{a}\left[\sqrt{(\xi^2-1)(1-\eta^2)}\xi\frac{\partial}{\partial\xi}-\sqrt{(\xi^2-1)(1-\eta^2)}\eta\frac{\partial}{\partial\eta}+i\,\frac{(\xi^2-\eta^2)}{\sqrt{(\xi^2-1)(1-\eta^2)}}\frac{\partial}{\partial\varphi}\right]|\chi_{\bar{\mu}_3}\rangle \\ &= \bar{a}\left[(\xi^2-1)^{\frac{M_3+1}{2}}\xi\frac{\partial}{\partial\xi}B_{i_n}^{k_3}e^{i\varphi}(1-\eta^2)^{1/2}Y_{l_n}^{M_3}(\xi^2-1)^{\frac{M_3+1}{2}}B_{i_n}^{k_3}\right. \\ &\quad\left.\times\left(e^{i\varphi}(1-\eta^2)^{1/2}\eta\frac{\partial}{\partial\eta}+\frac{M_3e^{i\varphi}\eta^2}{(1-\eta^2)^{1/2}}\right)Y_{l_n}^{M_3}\right]. \end{aligned} \tag{A6}$$

For $n=4$ component:

$$\begin{aligned} (p_x-ip_y)|\chi_{\bar{\mu}_4}\rangle &= -ie^{-i\varphi}\,\bar{a}\left[\sqrt{(\xi^2-1)(1-\eta^2)}\xi\frac{\partial}{\partial\xi}-\sqrt{(\xi^2-1)(1-\eta^2)}\eta\frac{\partial}{\partial\eta}-i\,\frac{(\xi^2-\eta^2)}{\sqrt{(\xi^2-1)(1-\eta^2)}}\frac{\partial}{\partial\varphi}\right]|\chi_{\bar{\mu}_4}\rangle \\ &= \bar{a}\left[\left((\xi^2-1)^{\frac{M_4}{2}}\xi\frac{\partial}{\partial\xi}B_{i_n}^{k_4}+2M_4(\xi^2-1)^{\frac{M_4-1}{2}}\xi^2B_{i_n}^{k_4}\right)e^{-i\varphi}(1-\eta^2)^{1/2}Y_{l_n}^{M_4}-(\xi^2-1)^{\frac{M_4+1}{2}}\right. \\ &\quad\left.\times B_{i_n}^{k_4}\left(e^{i\varphi}(1-\eta^2)^{1/2}\eta\frac{\partial}{\partial\eta}Y_{l_n}^{M_4}-\frac{M_4e^{i\varphi}\eta^2}{(1-\eta^2)^{1/2}}Y_{l_n}^{M_4}\right)\right]. \end{aligned} \tag{A7}$$

A.3. Application of the two-center potential operator:
For $n=1$ and $n=2$ components:

$$\begin{aligned} V_{\rm TC}|\chi_{\mu_n}\rangle &= -\bar{a}\left[(Z_1+Z_2)\xi+(Z_2-Z_1)\eta\right]|\chi_{\mu_n}\rangle \\ &= -\bar{a}\left[(Z_1+Z_2)\xi(\xi^2-1)^{|M_n|/2}B_{i_n}^{k_n}\,Y_{l_n}^{M_n}+(Z_2-Z_1)(\xi^2-1)^{|M_n|/2}B_{i_n}^{k_n}\,\eta Y_{l_n}^{M_n}\right]. \end{aligned} \tag{A8}$$

For $n=3$ and $n=4$ components:

$$\begin{aligned} V_{\rm TC}|\chi_{\bar{\mu}_n}\rangle &= -\bar{a}\left[(Z_1+Z_2)\xi+(Z_2-Z_1)\eta\right]|\chi_{\bar{\mu}_n}\rangle \\ &= -\bar{a}\left[(Z_1+Z_2)\xi(\xi^2-1)^{|M_n|/2}B_{i_n}^{k_n}\,Y_{l_n}^{M_n}+(Z_2-Z_1)(\xi^2-1)^{|M_n|/2}B_{i_n}^{k_n}\,\eta Y_{l_n}^{M_n}\right]. \end{aligned} \tag{A9}$$

A.4. Application of the energy re-scaling on the basis set elements:
For $n = 1$ and $n = 2$ components:

$$(mc^2 - E)|\chi_{\mu_n}\rangle = (mc^2 - E)(\xi^2 - 1)^{|M_n|/2} B_{i_n}^{k_1} Y_{l_n}^{M_n}. \tag{A10}$$

For $n = 3$ and $n = 4$ components:

$$(mc^2 + E)|\chi_{\bar{\mu}_n}\rangle = i\,(mc^2 + E)(\xi^2 - 1)^{|M_n|/2} B_{i_n}^{k_1} Y_{l_n}^{M_n}. \tag{A11}$$

[1] C. Feng and H. Deng, Review of fully coherent free-electron lasers, Nucl. Sci. Tech. **29**, 160 (2018).
[2] G. Zhaohe, et. al., Experimental demonstration of attosecond pump-probe spectroscopy with an X-ray free-electron laser (2024), arXiv:2401.15250 [physics.acc-ph].
[3] T. Driver, et.al., Attosecond delays in X-ray molecular ionization, Nature **632**, 762 (2024).
[4] F. Zapata, et.al., B-spline solution of the two-center Dirac equation in the electronic continuum for relativistic molecular photoionization, J. Chem. Theory Comput. **20**, 10507 (2024), https://doi.org/10.1021/acs.jctc.4c01232.
[5] T. Saue, R. Bast, A. S. P. Gomes, H. J. A. Jensen, L. Visscher, I. A. Aucar, R. Di Remigio, K. G. Dyall, E. Eliav, E. Fasshauer, T. Fleig, L. Halbert, E. D. Hedegård, B. Helmich-Paris, M. Iliaš, C. R. Jacob, S. Knecht, J. K. Laerdahl, M. L. Vidal, M. K. Nayak, M. Olejniczak, J. M. H. Olsen, M. Pernpointner, B. Senjean, A. Shee, A. Sunaga, and J. N. P. van Stralen, The dirac code for relativistic molecular calculations, The Journal of Chemical Physics **152**, 204104 (2020).
[6] T. Shiozaki, Bagel: Brilliantly advanced general electronic-structure library, WIREs Computational Molecular Science **8**, e1331 (2018).
[7] E. J. Baerends, N. F. Aguirre, N. D. Austin, J. Autschbach, F. M. Bickelhaupt, R. Bulo, C. Cappelli, A. C. T. van Duin, F. Egidi, C. Fonseca Guerra, A. Förster, M. Franchini, T. P. M. Goumans, T. Heine, M. Hellström, C. R. Jacob, L. Jensen, M. Krykunov, E. van Lenthe, A. Michalak, M. M. Mitoraj, J. Neugebauer, V. P. Nicu, P. Philipsen, H. Ramanantoanina, R. Rüger, G. Schreckenbach, M. Stener, M. Swart, J. M. Thijssen, T. Trnka, L. Visscher, A. Yakovlev, and S. van Gisbergen, The amsterdam modeling suite, The Journal of Chemical Physics **162**, 162501 (2025).
[8] C. Froese Fischer and O. Zatsarinny, A b-spline galerkin method for the dirac equation, Computer Physics Communications **180**, 879 (2009).
[9] V. M. Shabaev, I. I. Tupitsyn, V. A. Yerokhin, G. Plunien, and G. Soff, Dual kinetic balance approach to basis-set expansions for the dirac equation, Phys. Rev. Lett. **93**, 130405 (2004).
[10] A. N. Artemyev, A. Surzhykov, P. Indelicato, G. Plunien, and T. Stöhlker, Finite basis set approach to the two-centre dirac problem in cassini coordinates, Journal of Physics B: Atomic, Molecular and Optical Physics **43**, 235207 (2010).
[11] C. F. Fischer and F. A. Parpia, Accurate spline solutions of the radial dirac equation, Physics Letters A **179**, 198 (1993).
[12] A. Igarashi, B-spline expansions in radial dirac equation, Journal of the Physical Society of Japan **75**, 114301 (2006).
[13] A. Igarashi, Kinetically balanced b-spline expansions in radial dirac equation, Journal of the Physical Society of Japan **76**, 054301 (2007).
[14] K. Beloy and A. Derevianko, Application of the dual-kinetic-balance sets in the relativistic many-body problem of atomic structure, Computer Physics Communications **179**, 310 (2008).
[15] F. m. c. Fillion-Gourdeau, E. Lorin, and A. D. Bandrauk, Numerical solution of the time-independent dirac equation for diatomic molecules: b splines without spurious states, Phys. Rev. A **85**, 022506 (2012).
[16] E. B. Rozenbaum, D. A. Glazov, V. M. Shabaev, K. E. Sosnova, and D. A. Telnov, Dual-kinetic-balance approach to the dirac equation for axially symmetric systems: Application to static and time-dependent fields, Phys. Rev. A **89**, 012514 (2014).
[17] I. I. Tupitsyn and D. V. Mironova, Relativistic calculations of ground states of single-electron diatomic molecular ions, Optics and Spectroscopy **117**, 351 (2014).
[18] F. Fillion-Gourdeau, E. Lorin, and A. Bandrauk, Galerkin method for unsplit 3-d dirac equation using atomically/kinetically balanced b-spline basis, Journal of Computational Physics **307**, 122 (2016).
[19] W. Hahn, A. N. Artemyev, and A. Surzhykov, Improvement of the basis for the solution of the dirac equation in cassini coordinates, Optics and Spectroscopy **123**, 225 (2017).
[20] S. K. Luke, G. Hunter, R. P. McEachran, and M. Cohen, Relativistic Theory of H_2^+, The Journal of Chemical Physics **50**, 1644 (1969).
[21] V. A. Lyul'ka, Quantum-mechanical two-center problem for the dirac equation, Theoretical and Mathematical Physics **28**, 737 (1976).
[22] B. Müller and W. Greiner, The two centre dirac equation, Zeitschrift für Naturforschung A **31**, 1 (1976).
[23] W. D. Sepp, D. Kolb, W. Sengler, H. Hartung, and B. Fricke, Relativistic dirac-fock-slater program to calculate potential-energy curves for diatomic molecules, Phys. Rev. A **33**, 3679 (1986).
[24] N. Toshima and J. Eichler, Coupled-channel theory of excitation and charge transfer in relativistic atomic collisions, Phys. Rev. A **38**, 2305 (1988).
[25] K. Momberger, N. Grun, and W. Scheid, Non-

perturbative character of bound-free electron-positron pair production and the role of phase-distortion effects, Journal of Physics B: Atomic, Molecular and Optical Physics **26**, 1851 (1993).
[26] K. Rumrich, G. Soff, and W. Greiner, Ionization and pair creation in relativistic heavy-ion collisions, Phys. Rev. A **47**, 215 (1993).
[27] J. Eichler and W. Meyerhof, *Relativistic Atomic Collisions* (Academic Press, 1995).
[28] K. Schulze, J. Anton, W.-D. Sepp, and B. Fricke, Energy dependence of the molecular-orbital x-ray interference structure in U^{92+} − Pb collsions, Phys. Rev. A **58**, 1578 (1998).
[29] M. Gail, N. Grün, and W. Scheid, Coupled channel calculations for electron–positron pair production in collisions of heavy ions1, Journal of Physics B: Atomic, Molecular and Optical Physics **36**, 1397 (2003).
[30] U. Becker, N. Grün, W. Scheid, and G. Soff, Nonperturbative Treatment of Excitation and Ionization in U^{92+} + U^{91+} Collisions at 1 GeV/amu, Phys. Rev. Lett. **56**, 2016 (1986).
[31] M. R. Strayer, C. Bottcher, V. E. Oberacker, and A. S. Umar, Lattice calculation of muon-pair production with capture in relativistic heavy-ion collisions, Phys. Rev. A **41**, 1399 (1990).
[32] J. Thiel, A. Bunker, K. Momberger, N. Grün, and W. Scheid, Electron-positron pair creation with capture and ionization in relativistic heavy-ion collisions by the finite-difference method, Phys. Rev. A **46**, 2607 (1992).
[33] K. Momberger, A. Belkacem, and A. H. So/rensen, Numerical treatment of the time-dependent dirac equation in momentum space for atomic processes in relativistic heavy-ion collisions, Phys. Rev. A **53**, 1605 (1996).
[34] J. C. Wells, V. E. Oberacker, M. R. Strayer, and A. S. Umar, Convergence of a lattice calculation for bound-free muon-pair production in peripheral relativistic heavy-ion collisions, Phys. Rev. A **53**, 1498 (1996).
[35] O. Kullie and D. Kolb, High accuracy Dirac-finite-element (FEM) calculations for H_2^+ and Th_2^{179+}, The European Physical Journal D - Atomic, Molecular, Optical and Plasma Physics **17**, 167 (2001).
[36] D. C. Ionescu and A. Belkacem, Dynamics of ionization mechanisms in relativistic collisions involving heavy and highly-charged ions, The European Physical Journal D - Atomic, Molecular, Optical and Plasma Physics **18**, 301 (2002).
[37] O. Busic, N. Grün, and W. Scheid, Calculations for electron transitions on a three-dimensional lattice in relativistic heavy-ion collisions, Phys. Rev. A **70**, 062707 (2004).
[38] M. Y. Şengül, M. C. Güçlü, and S. Fritzsche, Bound-free electron-positron pair production in relativistic heavy-ion collisions, Phys. Rev. A **80**, 042711 (2009).
[39] A. A. Kotov, D. A. Glazov, V. M. Shabaev, and G. Plunien, One-electron energy spectra of heavy highly charged quasimolecules: Finite-basis-set approach, Atoms **9**, 10.3390/atoms9030044 (2021).
[40] O. Kullie and S. Schiller, Solution of the two-center dirac equation with 20-digit precision using the finite-element technique, Phys. Rev. A **105**, 052801 (2022).
[41] H. D. Nogueira, V. I. Korobov, and J.-P. Karr, High-precision solution of the dirac equation for the hydrogen molecular ion by an iterative method, Phys. Rev. A **105**, L060801 (2022).
[42] H. D. Nogueira and J.-P. Karr, High-precision solution of the dirac equation for the hydrogen molecular ion using a basis-set expansion, Phys. Rev. A **107**, 042817 (2023).
[43] C. M. König, M. Bohman, F. Heiße, J. Morgner, T. Sailer, B. Tu, K. Blaum, S. Sturm, D. Bakalov, H. D. Nogueira, J.-P. Karr, O. Kullie, and S. Schiller, High-precision penning trap spectroscopy of the ground state spin structure of hd^+, Phys. Rev. Lett. **136**, 143002 (2026).
[44] M. Brosolo and P. Decleva, Variational approach to continuum orbitals in a spline basis: An application to H_2^+ photoionization, Chem. Phys. **159**, 185 (1992).
[45] M. Brosolo, P. Decleva and A. Lisini, Accurate variational determination of continuum wavefunctions by a one-centre expansion in a spline basis. An application to H_2^+ and HeH^{2+} photoionization, J. Phys. B **25**, 3345 (1992).
[46] H. Bachau, E. Cormier, P. Decleva, J. E. Hansen, and F. Martín, Applications of B-splines in atomic and molecular physics, Reports on Progress in Physics **64**, 1815 (2001).
[47] H. Margenau and G. Murphy, *The Mathematics of Physics and Chemistry* (D. Van Nostrand Company, Incorporated, 1949).
[48] W. Greiner, *Relativistic quantum mechanics: Wave equations* (Springer, 2000).
[49] I. P. Grant, *Relativistic Quantum Theory of Atoms and Molecules: Theory and Computation (Springer Series on Atomic, Optical, and Plasma Physics)* (Springer-Verlag, Berlin, Heidelberg, 2006).
[50] H.A. Bethe and E.E. Salpeter, *Quantum Mechanics of One- and Two-Electron Atoms* (Springer Berlin Heidelberg, 2013).
[51] F. Zapata, J. M. Dahlström, A. Ljungdahl, E. Lindroth and J. Vinbladh, Relativistic time-dependent configuration-interaction singles method, Phys. Rev. A **105**, 012802 (2022).
[52] I. J. Schoenberg, Contributions to the problem of approximation of equidistant data by analytic functions, in *I. J. Schoenberg Selected Papers*, edited by C. de Boor (Birkhäuser Boston, Boston, MA, 1988) pp. 3–57.
[53] C. de Boor, *A practical guide to splines* (Springer-Verlag, New York, 1978).
[54] L. Argenti and R. Colle, On the b-splines effective completeness, Computer Physics Communications **180**, 1442 (2009).
[55] W. H. Press, S. A. Teukolsky, W. T. Vetterling, and B. P. Flannery, *Numerical Recipes 3rd Edition: The Art of Scientific Computing*, 3rd ed. (Cambridge University Press, USA, 2007).
[56] A. Edmonds, *Angular Momentum in Quantum Mechanics*, Investigations in Physics Series (Princeton University Press, 1996).
[57] M. Abramowitz and I. A. Stegun, *Handbook of Mathematical Functions with Formulas, Graphs, and Mathematical Tables* (Dover, New York, 1964).
[58] H. Margenau and G.M. Murphy, *Mathematics of Physics and Chemistry* (D. Von Nostrand Company Inc., 1946).